

Local Interstellar Matter: The Apex Cloud

Priscilla C. Frisch

*University of Chicago, Department of Astronomy and Astrophysics, 5460 S. Ellis Avenue,
Chicago, IL 60637*

ABSTRACT

Several nearby individual low column density interstellar cloudlets have been identified previously based on kinematical features evident in high-resolution Ca^+ observations near the Sun. One of these cloudlets, the ‘Apex Cloud’ (AC), is within 5 pc of the Sun in the solar apex direction. The question of which interstellar cloud will constitute the next galactic environment of the Sun in principle can be determined from cloudlet velocities. The interstellar absorption lines towards α Cen (the nearest star) are consistent within measurement uncertainties with the projected G-cloud (GC) and AC velocities, and also with the velocity of the cloud inside of the solar system (the Local Interstellar Cloud, LIC) providing a small velocity gradient is present in the LIC. The high GC column density towards α Oph compared to α Aql suggests that α Aql may be embedded in the GC so that the AC would be closer to the Sun than the GC. This scenario favors the AC as the next cloud to be encountered by the Sun, and the AC would have a supersonic velocity with respect to the LIC. The weak feature at the AC velocity towards 36 Oph suggests that the AC cloud is either patchy or does not extend to this direction. Alternatively, if the GC is the cloud which is foreground to α Cen, the similar values for $N(\text{H}^\circ)$ in the GC components towards α Cen and 36 Oph indicates this cloud is entirely contained within the nearest ~ 1.3 pc, and the Ca^+ GC data towards α Oph would then imply a cloud volume density of $\sim 5 \text{ cm}^{-3}$, with dramatic consequences for the heliosphere in the near future.

Subject headings: ISM: clouds, structure

1. Introduction

The interstellar material (ISM) within ~ 30 parsecs of the Sun is one of the few regions of the Milky Way Galaxy where there is a reasonable possibility of separating the effects of

topology and kinematics, and also identifying the properties of sub-parsec sized cloudlets. Velocities of interstellar absorption lines seen towards nearby stars tag cloudlets, and give advance warning of variations in the solar galactic environment. Interstellar material inside of the solar system was first identified by a weak $L\alpha$ interplanetary glow from the resonance fluorescence of solar $L\alpha$ emission scattering from interstellar H° inside of the solar system (e.g. Bertaux & Blamont 1971; Thomas & Krassa 1971). The astronomical identification of this cloud was difficult, however, since *Copernicus* satellite observations of the interplanetary $L\alpha$ glow showed that nearby ISM towards Scorpius and Ophiuchus stars has a different velocity than the interstellar H° inside of the solar system (Adams & Frisch 1977). Presently, the best determination of the velocity vector of ISM inside of the solar system (or the Local Interstellar Cloud, LIC) is derived from direct Ulysses observations of interstellar He° inside of the solar system, and EUVE observations of the He° 584 Å backscattered emission (Witte et al. 2003; Flynn et al. 1998, Table 1). These data give a LIC velocity of -26.3 ± 0.4 km s $^{-1}$ (all velocities here are heliocentric unless specifically identified as in the local standard of rest, LSR). The heliocentric upstream direction is $l^{II}=3.4 \pm 0.5^{\circ}$, $b^{II}=15.9 \pm 0.5^{\circ}$. This corresponds to an LSR velocity vector of -15.8 km s $^{-1}$ from an upstream direction $l^{II}=346^{\circ}$, $b^{II}=0.2^{\circ}$.¹ Other cloudlets besides the LIC are close to the Sun. Interstellar absorption line velocities towards α CMa (2.7 pc) and α Aql (5 pc) give evidence for about one cloud per 1.5 pc (e.g. Lallement et al. 1995). The Sun moves with respect to the LIC at ~ 5 pc per million years, and should enter a new cloud within the next $\sim 200,000$ years. This letter explores which of these cloudlets within 5 pc of the Sun is likely to form the next galactic environment of the Sun.

The first step in understanding the small-scale structure of nearby ISM requires using cloud kinematics to identify individual cloudlets. Optical Ca^{+} lines show nearby ISM flows past the Sun with an upstream direction indicating an origin associated with the Scorpius-Centaurus Association, and discrete cloudlets are identified in this flow (e.g. Frisch 1981; Crutcher 1982; Bzowski 1988; Frisch & York 1986; Crawford 1991; Frisch 1995; Vallerga et al. 1993; Lallement et al. 1986, LVF86). The Ca^{+} studies are heavily weighted towards gas in the upstream direction (the galactic hemisphere) since interstellar Ca^{+} is extremely difficult to observe towards the downstream stars because of low column densities. The velocity difference between upstream interstellar gas and the LIC developed into a paradigm for describing the velocities of nearby ISM in terms of two clouds, the 'G' Cloud (GC) towards the galactic center hemisphere, and the LIC (Lallement et al. 1990; Lallement & Bertin 1992,

¹For converting the derived heliocentric vectors to the Local Standard of Rest (LSR), the solar apex motion based on *Hipparcos* data is used, corresponding to a velocity $V=13.4$ km s $^{-1}$, towards $l^{II}=27.7^{\circ}$ and $b^{II}=32.4^{\circ}$ (Dehnen & Binney 1998).

LB92). The GC (with heliocentric velocity $-29.4 \pm 0.5 \text{ km s}^{-1}$) was derived from observations of a group of stars between $l^{\text{II}}=200^\circ \rightarrow 60^\circ$, $b^{\text{II}}=-70^\circ \rightarrow 40^\circ$ (Lallement et al. 1990), however many stars in this region do not show components at the GC velocity (Crawford 2001).

An analysis of ~ 100 interstellar Ca^+ and ultraviolet absorption components observed towards 60 nearby stars indicates that nearby ISM consists of a group of cloudlets flowing with bulk flow velocity $V(\text{BF})=-28.1 \pm 4.6 \text{ km s}^{-1}$, from an upstream direction towards the Scorpius-Ophiuchus Association (Frisch et al. 2002; Frisch 1995, Paper I, Table 1). In Paper I, we numerically filtered data in the data set used for the analysis in order to minimize the possibility of misidentified circumstellar components. GC components were subsumed in the bulk flow vector, rather than identified as a single distinct cloud. Many of the absorption components were found to be grouped into individual (5–7) kinematical and spatial groups in the rest frame of the bulk flow (reminiscent of the LVF02 cloudlets). One of these groups, identified as the “Aql-Oph” cloud in Paper I and as “Panoromix” in LVF86, is close to the solar apex motion and is here termed the “Apex Cloud” (AC). The AC, seen towards α Aql, is close to the Sun and a candidate for the next interstellar cloud to be encountered by the Sun.

The analysis method used here is discussed in Paper I. The data are from Paper I, supplemented by Mg^+ velocity data from Redfield & Linsky (2002, RL02), including the addition of data on the stars ξ BooA, $\chi 1$ Ori, κ^1 Cet, AU Mic, HZ 43, 101 Tau, and γ Dra.

2. Clouds

2.1. Apex Cloud

In Paper I, the AC cloud was identified towards 5 stars, α Aql, α Oph, ζ Aql, γ Oph, and λ Aql, and possibly towards δ Cyg (although the component is cold, $b(\text{Na}^\circ)=0.42 \text{ km s}^{-1}$, unlike other nearby components Welty et al. 1994). Since the AC must be within 5 pc, it is reasonable to ask if it is also in front of α Cen. This possibility is tested here by rederiving the AC velocity vector, using the original 5 stars sampling the Aql-Oph cloud and the Mg^+ line velocity in α CenA,B (RL02). The resulting best-fit vector, $V(\text{AC})$, shows that the α CenA,B and the Aql-Oph components have a velocity consistent with a single velocity vector. A component was deemed consistent if $|dV_i| \lesssim 1.3 \text{ km s}^{-1}$, where dV_i is the difference between the observed component velocity (not including uncertainties) and the projected best-fit $V(\text{AC})$ velocity for star i . In an iterative process, this best-fit velocity vector was then used to search for other consistent velocity components with $dV_i \lesssim 1.3 \text{ km s}^{-1}$, and then rederived. The final best-fit vector (Table 1) is based on 15 stars in the galactic center hemisphere,

including the -35 km s^{-1} component towards 36 Oph (see below). The fit is robust in the sense that the omission of either 36 Oph or two second quadrant (90° – 180°) AC components from the fitted sample yields a best fit AC vector differing by $<0.2 \text{ km s}^{-1}$ and $<0.3^\circ$ from the quoted value. The LSR AC vector corresponds to a velocity $-23.3 \pm 0.5 \text{ km s}^{-1}$, from the LSR upstream direction $l^{\text{II}}=5.5^\circ$, $b^{\text{II}}=4.1^\circ$. The heliocentric AC vector derived here is close to the value found for the “Panoromix” cloud in LVF86. Table 2 lists the components with $|dV_i(\text{AC})| \lesssim 1.3 \text{ km s}^{-1}$ for stars in the galactic center hemisphere. Fig. 1 shows that stars with $|dV_i(\text{AC})| < 1.3 \text{ km s}^{-1}$ at the AC velocity (circles) are found predominantly in or close to the galactic center hemisphere, although AC components in stars close to the shaded band (where $|dV_i(\text{AC}) - dV_i(\text{G})| < 2 \text{ km s}^{-1}$) may also be attributed to the GC (next section). The AC component (-19.6 km s^{-1}) towards α Pav (56 pc) is relatively cold, $T < 1,500 \text{ K}$ with $b(\text{Ca}^+) = 0.8 \text{ km s}^{-1}$ (Crawford et al. 1998). Cold components have not been observed in closer stars, and a serendipitous coincidence with the AC velocity can not be ruled out for any particular star, particularly more distant stars. The -35 km s^{-1} component towards 36 Oph is observed only as a weak broad H α feature, which Wood et al. (2000) attributed to an astrosphere around 36 Oph. The AC contribution, if present, would be blended with the astrosphere contribution, if real.

2.2. “G” Cloud

Although Ca^+ data show that components at the GC velocity are intermittent towards stars with adjacent sightlines (Crawford 2001), and the bulk flow of ISM past the Sun is consistent with a larger object (or shell) fragmented into cloudlets or filaments (Paper I), the assumption is made here that the GC is real. (The alternative assumption is that the GC components are a subset of the bulk flow vector, with a serendipitous coincidence in velocity.) The GC vector is then rederived in the same manner as the AC vector by fitting a best-fit vector through components in the stars α CenA,B, 36 Oph, α Aql, 70 Oph, and α Oph, and then searching for matching components in galactic center hemisphere stars. These matching components were refit for a better vector, yielding an LSR GC velocity of $-17.7 \pm 0.4 \text{ km s}^{-1}$ from an upstream direction $l^{\text{II}}=351.1^\circ$, $b^{\text{II}}=+8.5^\circ$. The heliocentric GC vector derived here is very close to the LB92 G vector (Table 1). The bulk velocity vector ($V(96)$, Table 1) of nearby cloudlets flowing past the Sun is also close to the G-cloud vector, since both derivations are based primarily on stars in the upstream direction where higher column densities make ground data more available. Stars showing components at the projected GC velocity (to within $|dV_i(\text{GC})| < 1.3 \text{ km s}^{-1}$) are plotted as crosses in Fig. 1.

2.3. LIC

For comparison, stars showing showing components at the projected LIC velocity, with $|dV_i(\text{LIC})| < 1.3 \text{ km s}^{-1}$, are plotted as crosses in Fig. 2. The LIC is generally well-defined in the downstream hemisphere ($l^{\text{II}}=90^\circ\text{--}270^\circ$). There is cluster of components at the LIC velocity, but probably unrelated to the LIC, near $l^{\text{II}}\sim 40^\circ$, $b^{\text{II}}=20\text{--}70^\circ$. The stars showing these components are in the tangential region of the Upper Centaurus-Lupus shell of the Scorpius-Centaurus superbubble, which has expanded to the solar vicinity (Frisch 1981; Crawford 1991; de Geus 1992; Frisch 1995). The nearest star in the group, HD 131156 ($l^{\text{II}}=23^\circ$, $b^{\text{II}}=61^\circ$), is 7 pc away.

3. Discussion

3.1. α Cen

One test of whether the AC or GC best describes the motion of the nearest upstream ISM constituting the future galactic environment of the Sun depends on the ISM component towards the nearest star α Cen. The GC fits the α CenAB component velocities best ($dV=-0.1, -0.4 \text{ km s}^{-1}$), although the AC also provides an excellent fit ($dV=0.6, 0.3 \text{ km s}^{-1}$). The apparent absence of a component at the LIC velocity towards α Cen has been a longstanding puzzle (Landsman et al. 1984). Hubble Space Telescope observations of Mg^+ and Fe^+ give a weighted mean interstellar gas velocity of $-18.0\pm 0.5 \text{ km s}^{-1}$ towards α CenAB, and a range -16.2 to -18.5 km s^{-1} when maximum reported measurement uncertainties are included (RL02). The projected LIC velocity vector towards α CenAB is -16.7 to -17.2 km s^{-1} , and the difference between the projected LIC velocity and the observed velocity ($dV < 1.0 \text{ km s}^{-1}$) is less than the reported (Linsky & Wood 1996) Doppler b -value (2.3 km s^{-1}), turbulent line broadening ($\sim 1.2 \text{ km s}^{-1}$), and nominal 3 km s^{-1} instrumental resolution. The data are consistent with the LIC filling the α Cen sightline, provided a small velocity gradient or discontinuity (e.g. $\simeq 0.5\text{--}1 \text{ km s}^{-1}$) is present in the cloud. The original conclusion that the upstream ISM velocity differs from the ISM velocity observed inside of the solar system was based on observations of the weak $\text{Ly}\alpha$ 1215 Å glow from solar radiation fluorescing on interstellar H° inside of the solar system (Adams & Frisch 1977; Lallement et al. 1990). However, the radiation pressure required to interpret the interplanetary $\text{Ly}\alpha$ glow was unknown for these early data, introducing large uncertainties in the analysis of the $\text{Ly}\alpha$ glow data. The improved He° LIC velocity reduced the discrepancy with the α Cen data. The small difference between the cloud temperature towards α Cen ($5,400\pm 500$, Linsky & Wood 1996) and the LIC ($6,300\pm 340$ K, Witte et al. 2003) is consistent with small temperature

gradients predicted by radiative transfer models for the LIC (Slavin & Frisch 2002). The GC and AC clouds both provide an acceptable fit to the α Cen, and the GC is the closest. The LIC also provides an acceptable fit if a small velocity gradient or discontinuity is present in the cloud. The explanation that the observed broadening of the α Cen Ly α absorption line due to the heating of H $^{\circ}$ in the outer heliosheath remains viable (Linsky & Wood 1996; Gayley et al. 1997).

3.2. The Apex Cloud versus G-Cloud as Future Environment of Sun

Since the current observational uncertainties do not allow the identity of the cloud towards α Cen AB to be firmly determined, α Cen can not be used to determine the next interstellar cloud to be encountered by the solar system. The stars α Aql, 36 Oph, 70 Oph, and α Oph provide the next set of tests as to whether the AC or GC (if it is real) will form the future solar environment. Fig. 1 shows that the nearest stars in the galactic center hemisphere tend to show components at both the GC and AC velocities, while more distant stars tend to show only the GC. Both the AC and GC are candidates for the next encountered cloud.

Component properties may help select whether the AC or GC is likely to be closer to the Sun. The high GC column density towards α Oph compared to α Aql suggests that α Aql is embedded in the GC, and that the AC is closer to the Sun than the GC. Towards 70 Oph the GC/AC ratio of $N(\text{Mg}^+)$ is ~ 23 (RL02), while the GC/AC ratios for $N(\text{Ca}^+)$ towards α Aql and α Oph are, respectively, 3 and 10. Thus the GC has significantly larger column densities than the AC. Both Mg^+ and Ca^+ are enhanced in the gas phase by grain destruction, so the larger GC column densities may signify a large cloud length, grain destruction (Frisch et al. 1999), or high volume densities. However, since α Cen and 36 Oph have comparable column densities (to within $\sim 15\%$, Linsky & Wood 1996; Wood et al. 2000), the large cloud length possibility is not viable. The extents of the AC and GC are shown in Fig. 1, indicating both clouds extend to the solar apex direction. Both clouds are patchy, and both clouds have an LSR upstream direction $\sim 40^\circ$ away from the solar apex direction (Table 1). Towards 36 Oph the AC component is barely detected, and was attributed originally to an astrosphere around 36 Oph (Wood et al. 2000). Towards α Oph, the GC is extremely patchy (Crawford 2001), which was originally attributed to the patchy H $^{\circ}$ 21 emission found at this velocity and in this region (Frisch et al. 1987).

The numerical quality of the fit of the AC and GC vectors to observed component velocities in stars in the galactic hemisphere is tested by plotting those components showing the smallest dV_i values ($\leq 1.3 \text{ km s}^{-1}$), for each star and each cloud. Fig. 3 shows a plot

of the minimum $dV_i(\text{AC})$ (x-axis) and the minimum $dV_i(\text{GC})$ (y-axis), for a star i . The dV_i values are determined after comparing $dV_i(\text{AC})$ and $dV_i(\text{GC})$ calculated for each component seen towards the star i (for an earlier version of this plot see Frisch 1997). If either the AC (or GC) vector perfectly described the velocity components in the galactic center hemisphere, the points would be lined up vertically (or horizontally) at 0 km/s. The scatter in dV_i values shows that neither velocity vector matches the data perfectly. Many of the stars showing a GC component are distant (Fig. 1), where a serendipitous coincidence in velocities is more likely. The dV standard deviations for the AC and GC components are, respectively, 0.7 km s^{-1} and 0.5 km s^{-1} , where only components used to derive the velocity vectors are included.

For comparison, the LIC components in the galactic center hemisphere are plotted in Fig. 4, where the y-axis is $dV_i(\text{LIC})$. The cluster of components at $dV_i(\text{AC}) \sim 6 \text{ km s}^{-1}$ and $dV_i(\text{LIC}) \sim 0 \text{ km s}^{-1}$ represent stars which sample the tangential region of the Upper Centaurus-Lupus superbubble (Fig. 2), and may coincidentally have the LIC velocity.

If the AC is the closest upstream cloud to the Sun, then the relative AC-Sun velocity $\sim 35 \text{ km s}^{-1}$, corresponding to ~ 35 parsecs per million years, suggests the AC is likely to replace the LIC as the next interstellar cloud surrounding the solar system sometime within the next $\sim 10^4$ – 10^5 years. The velocities of the AC (-35.0 km s^{-1}) and bulk flow velocity vectors (-28.1 km s^{-1}) differ by $\sim 25\%$, but the directions of the AC and bulk flow velocity vectors are within $\sim 8^\circ$ of each other. In this case, in the rest frame of the LIC the AC velocity AC is $\sim 10 \text{ km s}^{-1}$ and is close to the sound velocity (8.3 km s^{-1}) of a perfect gas at the LIC temperature ($\sim 6,300 \text{ K}$). This coincidence suggests that the kinematical structure of the nearest ISM may be related to sonic turbulence, and that a shock will form where the AC and LIC clouds collide. If the physical properties of the AC are similar to those of the LIC, the solar wind termination shock distance in the nose direction should decrease by $\sim 25\%$ (from simple equilibration of the solar wind and ISM ram pressures), which is comparable to variations expected from the solar cycle (e.g. Zank 1999; Tanaka & Washimi 1999; Scherer & Fahr 2003). In this case, the consequences for the inner heliosphere should be negligible. It is important to note in this context that $\sim 98\%$ of the diffuse material in the heliosphere today is ISM, although the inner heliosphere interplanetary medium is solar wind dominated because of the R^{-2} solar wind density dependence. If the colder α Pav component at the AC velocity is formed in the AC, the boundary conditions of the heliosphere may differ substantially from current values.

If instead the GC is the closest upstream cloud to the Sun, then the strongest observed nearby interstellar Ca^+ component, at the GC velocity towards α Oph, indicates that dramatic changes are in store for the heliosphere when it enters the GC within the next 10^3 – 10^5

years. The ratio $N(\text{Ca}^+)/N(\text{H}^\circ)$ in the GC would be $<7.1 \times 10^{-9}$, based on observations of the GC towards α Cen (Crawford 1994; Linsky & Wood 1996). This gives $N(\text{H}^\circ) > 2.3 \times 10^{19} \text{ cm}^{-2}$ for the GC component towards α Oph. This limit is close to $N(\text{H}^\circ)$ estimated for this component towards α Oph based on 21 cm data ($N(\text{H}^\circ) \leq 3.6 \times 10^{19} \text{ cm}^{-2}$ Frisch 1981). Since the GC $N(\text{H}^\circ)$ towards α Cen and 36 Oph are quite close, most of the GC density would be within 1.3 pc of the Sun, implying a GC density of $\geq 5 \text{ cm}^{-3}$ and future heliosphere shrinkage for possible cloud properties (Zank & Frisch 1999).

However the interpretation favored by this author, based on the above arguments and bias, is that the cloud order moving outwards from the Sun in the upstream direction consists of the LIC extending to virtually fill the α Cen sightline (with the required velocity gradient or discontinuity, which is consistent with the observed turbulence), followed by the AC which may or may not extend to the 36 Oph sightline, and beyond that the higher column density GC. The absence of the LIC towards 36 Oph would indicate a filamentary structure for the LIC. In this case the α Pav cold component at the AC velocity would be a serendipitous coincidence in velocities and unrelated to the AC. These derived cloud velocities, however, do not reflect these biases. High-resolution high-signal-to-noise spectroscopy of additional sightlines, particularly in the UV, are required to distinguish the correct interpretation of the data.

This research has been supported by NASA grants NAG5-8163, NAG5-11999, and NAG5-111005.

REFERENCES

- Adams, T. F. & Frisch, P. C. 1977, *ApJ*, 212, 300
- Bertaux, J. L. & Blamont, J. E. 1971, *A&A*, 11, 200
- Bzowski, M. 1988, *Acta Astronomica*, 38, 443
- Crawford, I. A. 1991, *A&A*, 247, 183
- . 1994, *The Observatory*, 114, 288
- . 2001, *MNRAS*, 327, 841
- Crawford, I. A., Lallement, R., & Welsh, B. Y. 1998, *MNRAS*, 300, 1181
- Crutcher, R. M. 1982, *ApJ*, 254, 82

- de Geus, E. J. 1992, *A&A*, 262, 258
- Dehnen, W. & Binney, J. J. 1998, *MNRAS*, 298, 387
- Flynn, B., Vallergera, J., Dalaudier, F., & Gladstone, G. R. 1998, *J. Geophys. Res.*, 103, 6483
- Frisch, P. & York, D. G. 1986, in *The Galaxy and the Solar System* (University of Arizona Press), 83–100
- Frisch, P. C. 1981, "Nature", 293, 377
- . 1995, *Space Sci. Rev.*, 72, 499
- Frisch, P. C. 1997, <http://xxx.lanl.gov/>, astroph/9705231
- Frisch, P. C., Dorschner, J. M., Geiss, J., Greenberg, J. M., Grün, E., Landgraf, M., Hoppe, P., Jones, A. P., Krätschmer, W., Linde, T. J., Morfill, G. E., Reach, W., Slavin, J. D., Svestka, J., Witt, A. N., & Zank, G. P. 1999, *ApJ*, 525, 492
- Frisch, P. C., Grodnicki, L., & Welty, D. E. 2002, *ApJ*, 574, 834
- Frisch, P. C., York, D. G., & Fowler, J. R. 1987, *ApJ*, 320, 842
- Gayley, K. G., Zank, G. P., Pauls, H. L., Frisch, P. C., & Welty, D. E. 1997, *ApJ*, 487, 259
- Lallement, R. & Bertin, P. 1992, *A&A*, 266, 479
- Lallement, R., Ferlet, R., Lagrange, A. M., Lemoine, M., & Vidal-Madjar, A. 1995, *A&A*, 304, 461
- Lallement, R., Ferlet, R., Vidal-Madjar, A., & Gry, C. 1990, in *Physics of the Outer Heliosphere*, 37–42
- Lallement, R., Vidal-Madjar, A., & Ferlet, R. 1986, *A&A*, 168, 225
- Landsman, W. B., Henry, R. C., Moos, H. W., & Linsky, J. L. 1984, *ApJ*, 285, 801
- Linsky, J. L. & Wood, B. E. 1996, *ApJ*, 463, 254
- Redfield, S. & Linsky, J. L. 2002, *ApJS*, 139, 439
- Scherer, K. & Fahr, H. 2003, *Geop. Res. Let.*, 30
- Slavin, J. D. & Frisch, P. C. 2002, *ApJ*, 565, 364
- Tanaka, T. & Washimi, H. 1999, *J. Geophys. Res.*, 104, 12605

- Thomas, G. E. & Krassa, R. F. 1971, *A&A*, 11, 218
- Vallerga, J. V., Vedder, P. W., Craig, N., & Welsh, B. Y. 1993, *ApJ*, 411, 729
- Welty, D. E., Hobbs, L. M., & Kulkarni, V. P. 1994, *ApJ*, 436, 152
- Witte, M., Banaszekiewicz, M., Rosenbauer, H., & McMullin, D. 2003, *Adv. Space Res.*, in press, 0000, 0000
- Wood, B. E., Linsky, J. L., & Zank, G. P. 2000, *ApJ*, 537, 304
- Zank, G. P. 1999, *Space Science Reviews*, 89, 413
- Zank, G. P. & Frisch, P. C. 1999, *ApJ*, 518, 965

Table 1. ISM Flows near the Sun

	HC Vector ^a			LSR Vector ^{a,b}			Notes
	Vel. (km s ⁻¹)	l (°)	b (°)	Vel (km s ⁻¹)	l (°)	b (°)	
Cloud surrounding solar system (LIC):							
$V(\text{He})$	-26.3 ± 0.4	3.6	15.3	-15.8	346.1	0.2	Witte et al. (2003) Flynn et al. (1998)
Bulk flow of nearby ISM:							
$V(96)$	-28.1 ± 4.6	12.4	11.6	-17.0	2.3	-5.2	60 stars (Frisch et al. 2002)
“G” Cloud:							
$V(\text{GC})$	-29.1 ± 0.5	5.3	+19.6	-17.7	351.2	+8.5	18 stars (this paper)
$V(\text{GC})$	-29.4 ± 0.4	4.5	+20.5	-18.0	350.0	+10.0	Lallement & Bertin (1992)
Apex Cloud:							
$V(\text{AC})$	-35.1 ± 0.6	12.7	14.6	-23.3 ± 0.5	5.5	4.1	15 stars (this paper)

^aGalactic coordinates correspond to upstream directions.

^bConversion to LSR uses the solar apex motion ($V=13.38$ km s⁻¹, towards galactic coordinates $l=27.7^\circ$, $b=32.4^\circ$) derived from Hipparcos data (Dehnen & Binney 1998).

Table 2. Stars in Galactic Center Hemisphere with Apex or G-Cloud Velocity Components^a

HD	Name	l	b	d	Spec.	AC Component		GC Component	
						Velocity km s ⁻¹	$dV(\text{AC})$ km s ⁻¹	Velocity km s ⁻¹	$dV(\text{GC})$ km s ⁻¹
		°	°	pc					
128620	α CenA	315.7	-0.7	1.4	G2 V	-17.8	0.6	s	-0.1
128621	α CenB	315.7	-0.7	1.4	K1 V	-18.1	0.3	s	-0.4
209100	ϵ Ind	336.2	-48.0	3.6	K4.5V	-9.2	-0.4
155886/5	36 OphAB	358.3	6.9	4.3	K0V/K1V	-35. :	-1.3	-27.9	0.3
187642	α Aql	47.7	-8.9	5.1	A7 V	-26.9	-0.7	-18.1	0.4
165341	70 Oph	29.9	11.4	5.1	K0V	-32.9	0.7	-26.6	-0.2
197481	AU Mic	12.7	-36.8	9.9	M0	-21.2	0.7
159561	α Oph	35.9	22.6	14.3	A5 III	-32.0	0.2	-26.2	-0.6
36705	AB Dor	275.3	-33.1	14.9	K1III	5.2	-0.2
115892	ι Cen	309.4	25.8	18.0	A2 V	-18.2	-0.6	s	-0.1
12311	α Hyi	289.5	-53.8	21.9	F0 V	4.9	0.1	s	1.0
177724	ζ Aql	46.9	3.3	25.5	A0 Vn	-29.7	-1.1	-20.6	0.5
161868	γ Oph	28.0	15.0	29.1	A0 V	-33.1	0.9
120418	θ Peg	67.4	-38.7	29.6	A2IV	-4.2	-0.3
209952	α Gru	350.0	-52.4	31.1	B7I V	-13.0	-0.9
88955	HR 4023	274.3	11.9	31.5	A2V	-1.7	-0.2
177756	λ Aql	30.3	-5.5	38.4	B9 Vn	-30.7	0.7
218045	α Peg	88.3	-40.4	42.8	B9III	-0.5	0.2
135742	β Lib	352.0	39.2	49.1	B8V	-26.9	0.0
160613	o Ser	13.3	9.2	51.5	A2Va	-29.0	-0.6
186882	δ Cyg	78.7	10.2	52.4	B9.5IV	-9.6	-0.1
193924	α Pav	340.9	-32.5	56.2	B2 IV	-19.6	0.0
213998	η Aqr	66.8	-47.6	56.3	B9IV-Vn	-2.1	-0.5
156928	ν Ser	10.6	13.5	59.3	A0/A1V	-27.7	1.2

^aThe velocities in columns 7 and 9 are the observed heliocentric component velocities. $dV(\text{AC})$ ($dV(\text{GC})$) is the difference between the observed and projected velocities of $V(\text{AC})$ ($V(\text{GC})$) in Table 1. The velocity references are given in Paper I (Ca⁺) and RL02 (Mg⁺). An “s” indicates the components listed in columns 7 and 9 are the same.

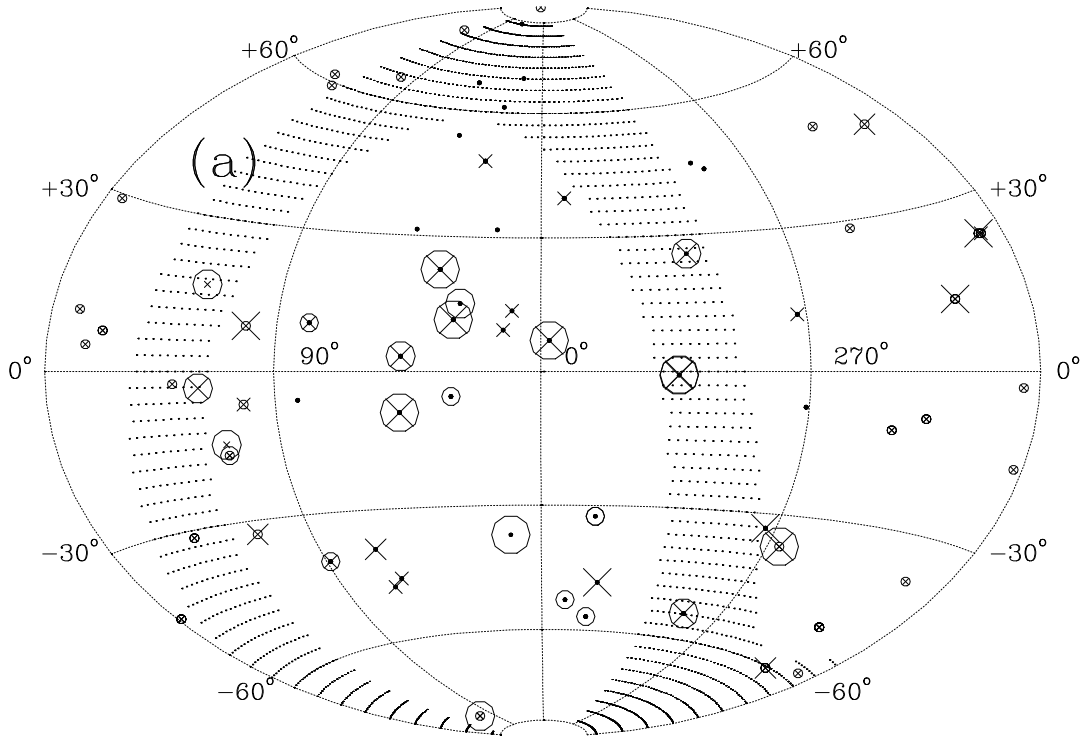


Fig. 1.— (a) Locations of stars showing a velocity absorption component with $|dV_i(\text{AC})| < 1.3$ km s^{-1} (circles) or $|dV_i(\text{GC})| < 1.3$ km s^{-1} (crosses). The regions where $|dV_i(\text{AC}) - dV_i(\text{GC})| < 2$ km s^{-1} are shaded. The size of the symbol is inversely related to the star distance. The plain dots show stars with no components at the AC or GC velocities.

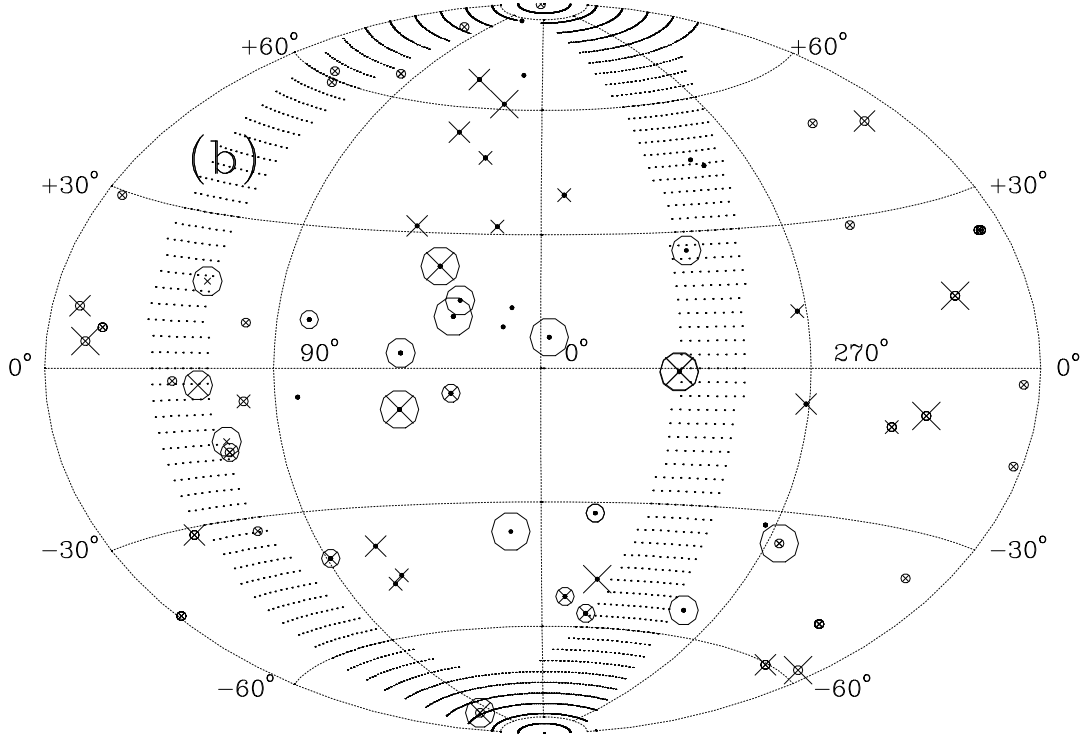


Fig. 2.— (b) Same as previous figure, except that the crosses are components at the LIC velocity and the shading is the overlap between the AC and LIC. The components at the LIC velocity near $l^{\text{II}} \sim 40^\circ$, $b^{\text{II}} = 20\text{--}70^\circ$ appear to sample a tangential region of the Upper Centaurus-Lupus shell of the Scorpius-Centaurus superbubble, which has expanded to the solar vicinity (Frisch 1981; Crawford 1991; de Geus 1992; Frisch 1995). The nearest star in the group, HD 131156 ($l^{\text{II}} = 23^\circ$, $b^{\text{II}} = 61^\circ$), is 7 pc away.

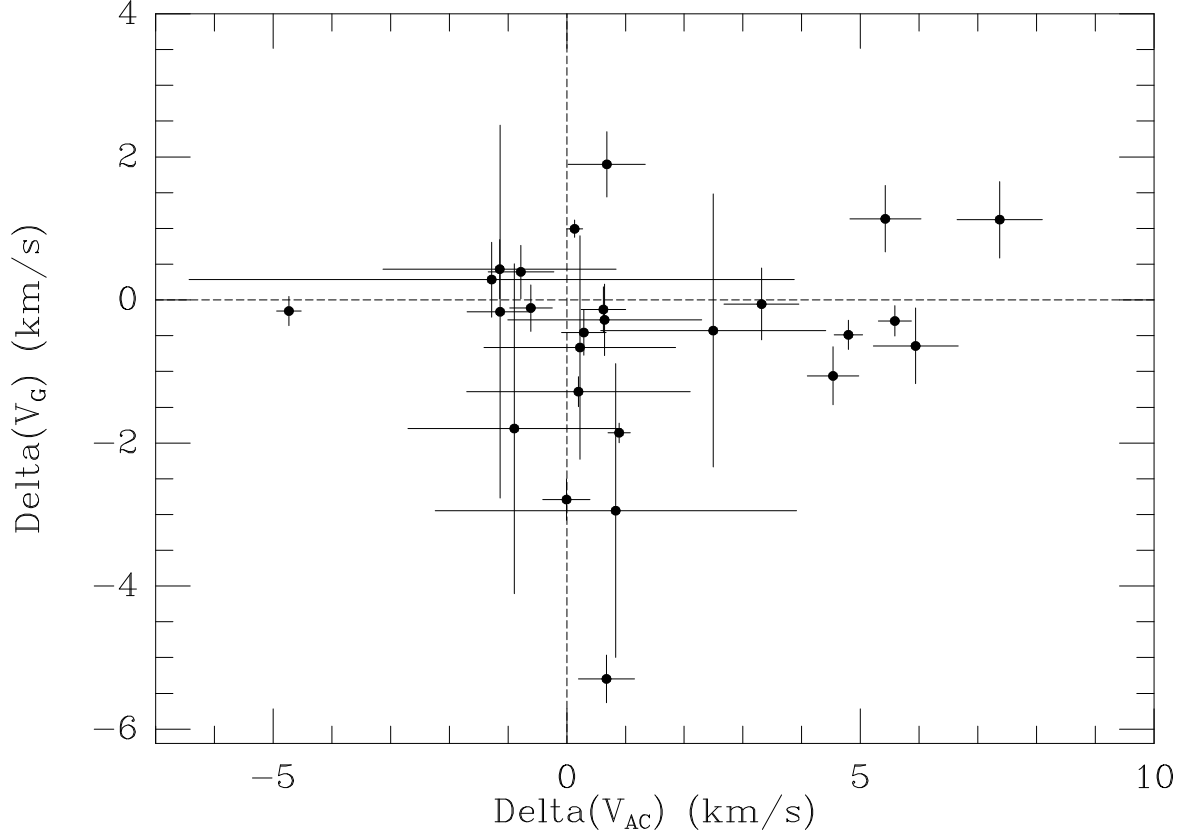


Fig. 3.— (a) This figure displays the ability of the AC and GC vectors to describe components seen towards each star in the galactic center hemisphere. The minimum $dV_i(AC)$ (x-axis) and the minimum $dV_i(GC)$ (y-axis) are plotted for each star. Where only one absorption component is present, $dV_i(AC)$ and $dV_i(GC)$ are calculated for the same component. Where several components are present for star i , the component with the minimum $dV_i(AC)$ value may be different from the component showing the minimum $dV_i(GC)$ value. If either the AC (or GC) vector perfectly described the velocity components in the galactic center hemisphere, the points would be lined up vertically (or horizontally) at 0 km/s. Stars with no matching components are omitted.

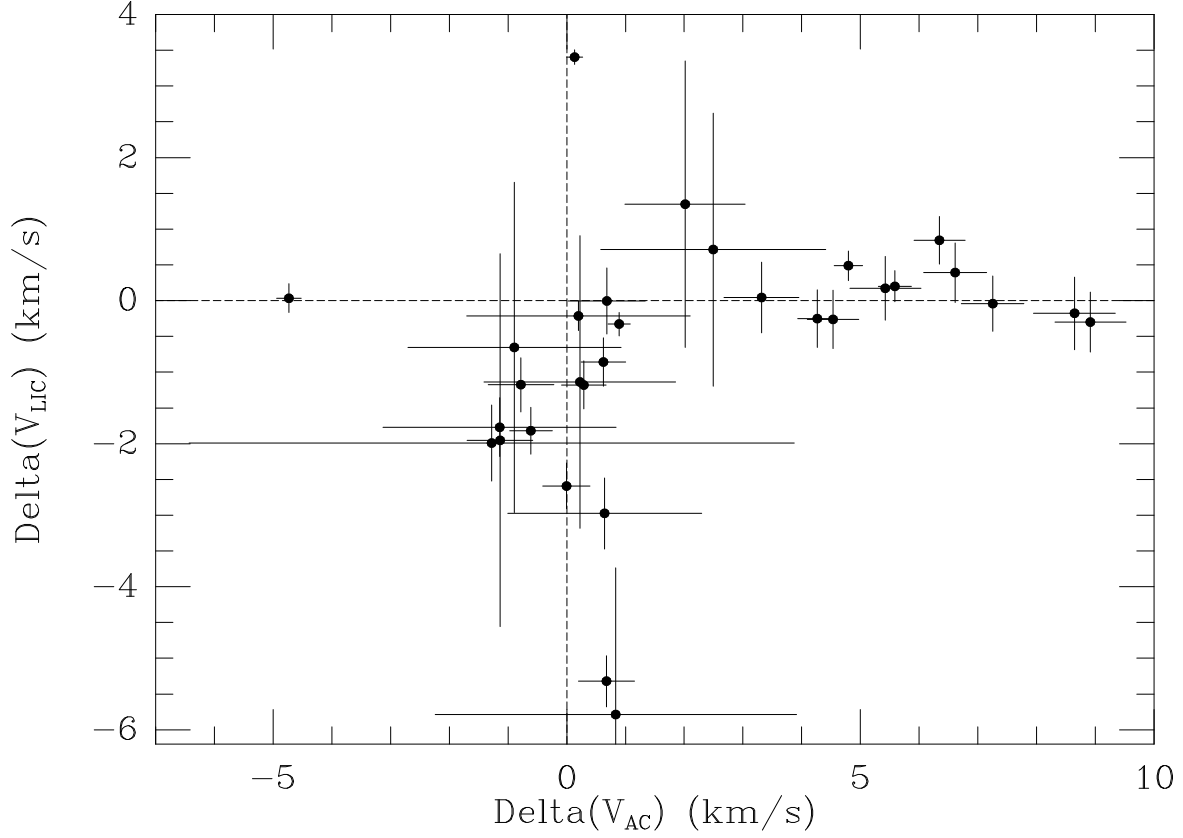


Fig. 4.— (b) Same as previous figure, except that the vertical scale displays components agreeing with the LIC velocity, for stars located in the galactic center hemisphere. The cluster of components at $dV_i(\text{AC}) \sim 6 \text{ km s}^{-1}$, $dV_i(\text{LIC}) \sim 0 \text{ km s}^{-1}$ appears to sample the tangential region of the Upper Centaurus-Lupus shell, noted in Fig. 2. If this component group is actually the LIC, the LSR upstream direction is towards $l^{\text{II}} \sim 346^\circ$, $b^{\text{II}} \sim 0^\circ$. Stars with no matching components are omitted.